Metal–Organic Frameworks

International Edition: DOI: 10.1002/anie.201908164
German Edition: DOI: 10.1002/ange.201908164

Atomic/Molecular Layer Deposited Iron–Azobenzene Framework Thin Films for Stimuli-Induced Gas Molecule Capture/Release

*Aida Khayyami, Anish Philip, and Maarit Karppinen**

Abstract: *The atomic/molecular layer deposition (ALD/MLD) technique provides an elegant way to grow crystalline metal–azobenzene thin films directly from gaseous precursors; the photoactive azobenzene linkers thus form an integral part of the crystal framework. Reversible water capture/release behavior for these thin films can be triggered through the trans–cis photoisomerization reaction of the azobenzene moieties in the structure. The ALD/MLD approach could open up new horizons for example, for the emerging fields of remotely controlled drug delivery and gas storage.*

Crystalline metal–organic networks such as the so-called coordination polymer (CP) and metal–organic framework (MOF) materials,[1–3] are intensively investigated for a vast arena of advanced applications, in particular those related to gas or drug molecule capture, storage, and delivery.[4–7] As an exciting option to widen the application horizon, adding a remote-controlled functionality could be imagined by introducing a stimuli-responsive component within the framework structure. Photostimulation is an attractive choice as light is a ubiquitous and sustainable resource, and moreover offers high spatial and temporal resolution.[8]

Azobenzene is the prototype of photoresponsive moieties; it undergoes a *trans–cis* isomerization from the thermodynamically more stable planar *trans* isomer to the aplanar *cis* form upon ultraviolet (UV) light irradiation. The back-switching is driven by visible light illumination or thermal relaxation.[9,10] Introduction of azobenzene moieties in porous MOF-like materials has already been challenged in recent studies.[11,12] These efforts can be divided into three groups depending on whether the azobenzene moiety is accommodated as 1) the actual framework linker,[13,14] 2) a side-group pendant to the linker,[15,16] or 3) a guest species in the pores incorporated either during the synthesis or through a post-synthesis treatment.[17,18] The first alternative would be truly exciting but difficult to realize; the challenges arise from the fact that azobenzene is an integral part of a rigid crystal structure in which the *trans–cis* transformation either does not occur owing to the lack of free space, or occurs but destroys the crystal lattice in an irreversible manner.[19–22]

A possible solution could be to fabricate the azobenzene-based metal–organic material in a polycrystalline form (preferably consisting of small crystallites) on top of a supporting substrate to allow more flexibility for the bond rearrangements during the isomerization.[23,24] An elegant way to achieve this could be to utilize the atomic/molecular layer deposition (ALD/MLD) fabrication technique. It yields the metal–organic material in high-quality thin-film form, thus allowing, as an additional bonus, the easy integration for example, with microelectronics device architectures.[25] In ALD/MLD the metal–organic material is grown from two mutually reactive gaseous precursors sequentially pulsed into the reactor chamber with an intermediate inert-gas purging step. Like in the case of the parent ALD (atomic layer deposition) technology for simple inorganic materials, this results in self-limited gas–surface reactions and consequently in the atomic/molecular level control of the growing thin-film material on the chosen substrate surface.[26,27] Most importantly, the recent advances have demonstrated that such an ALD/MLD process may yield in situ crystalline metal–organic thin films.[28–31]

Herein we report the ALD/MLD growth of crystalline iron–azobenzene thin films in which the azobenzene moieties are an integral part of the crystal framework. For this photoresponsive 3D network, we demonstrate the controlled capture and release of guest species using H_2O as a model guest. The films were deposited from $FeCl_3$ and azobenzene-4,4′-dicarboxylic acid precursors. We first optimized the deposition temperature for obtaining crystalline thin films in a controlled manner. The following ALD/MLD cycle was employed in these experiments: 4 s $FeCl_3$ pulse→8 s N_2 purge→30 s azobenzenedicarboxylic acid pulse→70 s N_2 purge. The temperature range investigated was 250–360 °C, the lower limit defined by the precursor sublimation temperatures (158 °C for $FeCl_3$, 240 °C for azobenzenedicarboxylic acid). Visually homogeneous films were obtained up to about 290 °C, after which not only the visual inhomogeneity but also the surface roughness increased such that the film thickness could not be determined any more by X-ray reflectivity (XRR) measurements, see Supporting Information for representative XRR and atomic force microscopy (AFM) data. Within the deposition temperature range of 250–290 °C, visually homogeneous in situ crystalline thin films were obtained. Within this temperature range the grazing-incidence X-ray diffraction (GIXRD) patterns for the films were essentially identical; in Figure 1 a we show a pattern recorded for a film deposited at 280 °C. The obtained GIXRD patterns could not be explained by any known metal–organic structure, thus underlining the fact that our iron–azobenzene films are of a new material.

It is practically impossible to solve the new crystal structure based on thin-film GIXRD data. Nevertheless, we

[*] A. Khayyami, Dr. A. Philip, Prof. M. Karppinen
Department of Chemistry and Materials Science, Aalto University
P.O. Box 16100, 00076 Aalto (Finland)
E-mail: maarit.karppinen@aalto.fi
Supporting information and the ORCID identification number(s) for the author(s) of this article can be found under: https://doi.org/10.1002/anie.201908164.

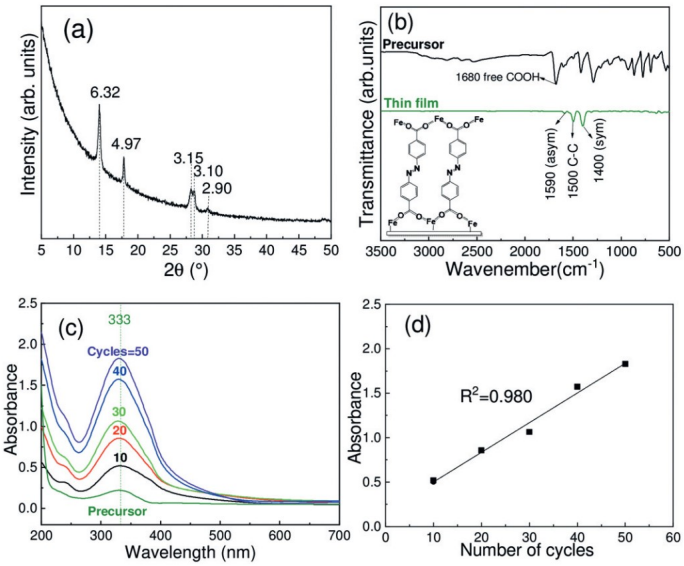

Figure 1. Basic characterization results for representative iron–azobenzene thin-film samples deposited at 280 °C: a) GIXRD pattern (peaks indicated with their d-values), b) FTIR spectrum (together with a spectrum for the azobenzenedicarboxylic acid precursor), c) UV/Vis absorption spectra for a set of thin films deposited with different numbers of ALD/MLD cycles (together with a spectrum for the azobenzenedicarboxylic acid precursor in aqueous solution), and d) absorbance at 333 cm^{-1} plotted against the number of ALD/MLD cycles.

can address the bonding structure in our iron–azobenzene films on the basis of their Fourier transform infrared (FTIR) spectra; in Figure 1b we show FTIR spectra both for a representative thin-film sample (deposited at 280 °C) and the azobenzene-4,4′-dicarboxylic acid precursor. Comparison of the two spectra confirms that upon the ALD/MLD surface reactions the azobenzenedicarboxylic acid precursor is bonded to Fe atoms through both the C=O and the OH groups of the carboxylic acid units to form a hybrid thin film of the $(Fe{-}O_2C{-}C_6H_4{-}N{=}N{-}C_6H_4{-}CO_2)_n$ type. This is revealed from the fact that both the broad absorption band around 3200–3500 cm^{-1} owing to the OH group and the sharp peak at 1680 cm^{-1} owing to the free carboxylic acid C=O stretching, which are readily identified for the precursor, are clearly non-existent in the spectrum of the iron–azobenzene thin film. Additionally, the splitting, that is, 190 cm^{-1}, between the symmetric and asymmetric carboxylate stretching peaks at 1400 and 1590 cm^{-1} suggests that the carboxylate bonding is of the bridging type[32] (see the sketch in Figure 1b). The peak at 1500 cm^{-1} is related to the aromatic-ring C–C stretch.[33]

To verify the presence of the azo N=N group in our hybrid thin films, we collected UV/Vis absorption spectra for a series of thin films (deposited at 280 °C) with different thicknesses and also for the azobenzenedicarboxylic acid precursor (in aqueous solution) for comparison (Figure 1c). The *trans* isomer of the azobenzene moiety exhibits a strong π–π* absorption peak around 333 nm, while for the *cis* isomer a weak (forbidden) n–π* band is expected at 550.[9] The spectra in Figure 1c unambiguously confirm the presence of the *trans* azobenzene moiety in our hybrid $(Fe{-}O_2C{-}C_6H_4{-}N{=}N{-}C_6H_4{-}CO_2)_n$ films. Another important observation is that the absorption band is identically located for both the azobenzenedicarboxylic acid precursor and all our hybrid thin films; this can be taken as an indication that the azobenzene moiety indeed is in the role of a linker directly coordinated to the metal atoms in the MOF structure.[34] Also, it is interesting to note as shown in Figure 1d that the absorbance at 333 nm increases linearly with the number of ALD/MLD cycles applied, in an excellent agreement with the ideally expected regular film growth.[35]

X-ray photoelectron spectroscopy (XPS) was employed to address the elemental composition and the oxidation state of iron in the films (see Supporting Information for details). The Fe 2p spectrum presents the characteristic Fe $2p_{3/2}$ and Fe $2p_{1/2}$ peaks at the binding energies of 711.6 and 725.6 eV, respectively. These values are typical for trivalent iron. Moreover, a distinct satellite peak appears at 718.4 eV, and the distance between the main peak and the satellite, that is, 6.8 eV, is another indication of the trivalent state of iron.[36–38] From the wide-scan spectrum, the presence of Fe, C, O, and N can be confirmed. Most importantly, the ratio N:Fe of about 2.6 (that is, azobenzene:Fe ratio of 1.3) is in accordance with a 5- or 6-fold coordination number for iron (taking into account the bridging-type bonding of each azobenzene moiety to four Fe atoms). The XPS data also reveal the presence of Cl contamination (ca. 1 at%), which is typical for ALD and MLD films grown from metal chloride precursors in particular at low deposition temperatures.[39,40]

Before investigating the guest absorption capability of the iron–azobenzene thin films, we elaborated our ALD/MLD process by optimizing the deposition parameters in more detail (see the Supporting Information). We confirmed that the growth-per-cycle (GPC) value, calculated from the XRR-determined film thickness and the number of ALD/MLD cycles applied, remained essentially constant at ca. 25 Å/cycle with increasing deposition temperature up to 290 °C (the films deposited at the higher temperatures became too rough for accurate thickness evaluation). Interestingly, the GPC value observed is quite high, being nearly twice the ideal length of one $(Fe{-}O_2C{-}C_6H_4{-}N{=}N{-}C_6H_4{-}CO_2)$ unit. Since our ALD/MLD process is well-controlled and highly reproducible, the high GPC value should not be due to any unideal growth mode. To show this we confirmed that the GPC value indeed saturates (as expected for an ideal ALD/MLD process) when the precursor pulse lengths exceed certain threshold limits (2.5 s for $FeCl_3$, 20 s for azobenzenedicarboxylic acid). For the rest of the experiments, we fixed the deposition temperature to 280 °C and the pulse/purge lengths as follows: 2.5 s $FeCl_3$/10 s N_2/20 s azobenzenedicarboxylic acid/50 s N_2. Under these conditions the film thickness increased with increasing number of ALD/MLD cycles in a highly linear manner.

Next we investigated the photoisomerization behavior of our iron–azobenzene thin films under irradiation by UV light (365 nm). For these measurements, the samples were grown on quartz substrates. It should be noted that the sample temperature in all experiments remained below 35 °C, as verified using a digital temperature controller. To investigate

the expected *trans–cis* photoisomerization reaction, we recorded the UV/Vis absorption spectrum in the wavelength range of 200–700 nm in 15 min time intervals during the UV illumination (Figure 2a). Irradiation with UV should excite the *trans*-azobenzene π–π* transition, followed by the *trans*-to-*cis* isomerization. This is what we can clearly see from Figure 2a, that is, a progressive decrease in the intensity of the π–π* band at 333 nm and an increase in the intensity of the n–π* band around 550 nm as an indication of the increase in the number of *cis* isomers.[35,41] We estimated[42] the portion of the *cis* azobenzene isomer to be ca. 6.3, 11.4, and 43.7 % after an irradiation period of 15, 30, and 300 min. Such a transformation rate is in line with observations made for example, for azobenzene-based covalent organic frameworks (COFs).[21,22]

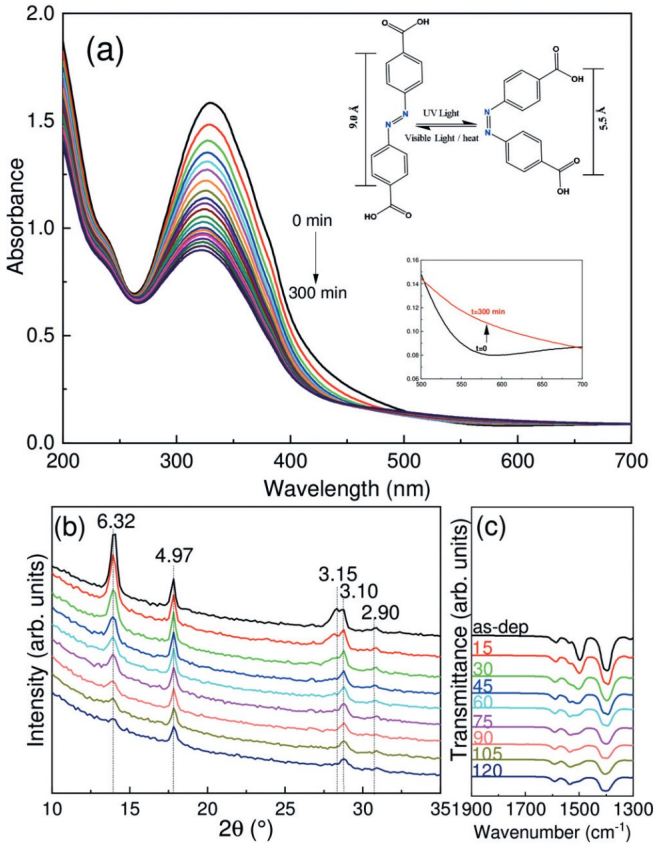

Figure 2. a) UV/Vis spectra, b) GIXRD patterns, and c) FTIR spectra recorded for a representative iron–azobenzene thin-film sample after UV (365 nm) irradiation for different time periods in intervals of 15 minutes.

We followed the photoisomerization reaction with GIXRD measurements as well, to learn the possible influence of the *trans*-to-*cis* transformation on the crystal structure of our iron–azobenzene thin films (Figure 2b). When the length of the irradiation period was increased, the diffraction peaks started to lose intensity, and at the same time the peaks became gradually broader, indicating a reduction in the degree of crystallinity/crystallite size upon the elongated irradiation. This is what might be expected when the planar *trans* isomer transforms to the less planar *cis* isomer, possibly enforcing folding of the structure and ultimately destructing the framework integrity.[11,21,22] However, for our iron–azobenzene thin films, no radical changes in the peak intensity/FWHM were seen within the first 30 minutes of irradiation. A detailed observation of the GIXRD patterns (Figure 2b) reveals that upon the photoisomerization the peak positions remain essentially unchanged; the only clearly visible change is the disappearance of the peak around $2\theta = 28.32$ ($d = 3.15$), indicating some change in crystal symmetry. From Figure 2c, where we show the FTIR spectra for the irradiated samples, a slight decrease in the intensity of the characteristic FTIR peaks owing to the azobenzene moiety can be seen, but only for the very long irradiation periods. Furthermore, it is notable that the shape of the band at 1500 cm^{-1} changes upon the UV irradiation; this has been interpreted as an indication of the presence of the *cis* conformation.[33]

Motivated by the possibility to utilize the photocontrolled isomerization reaction for the remote-controlled loading/release of gas molecules,[21] we designed a simple experiment to investigate the gas-absorption characteristics of our iron–azobenzene thin films. Water was chosen for the guest species as humidity treatments are easy to perform and the water absorption/desorption could be conveniently followed by FTIR measurements. We first confirmed that the iron–azobenzene structure is capable in absorbing water molecules. Then our aim was to clarify whether the *trans*-to-*cis* isomerization reaction can be used to trigger the water desorption from the water-absorbed films. In Figure 3a, we display representative FTIR spectra to illustrate the water absorption/desorption behavior of the films upon repeated humidity-treatment/UV-illumination cycles; the humidity treatment was carried out at room temperature for 48 hours under relative humidity of RH = 75 %. The broad peak appearing in the 3200–3500 cm^{-1} region after the humidity treatment is an indication of the water molecules in the structure. This peak disappears after the 15 min exposure to UV (365 nm) light, demonstrating that the water molecules are indeed detached from the structure upon the *trans*-to-*cis* isomerization. The reversibility was demonstrated by repeating the humidity-treatment/UV-illumination cycle three times (Figure 3a). Moreover, we confirmed that the loss of water upon UV

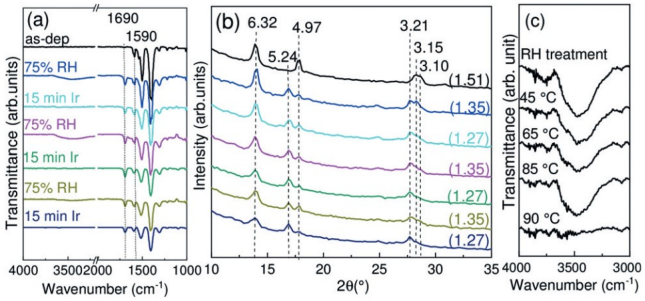

Figure 3. a) FTIR spectra and b) GIXRD patterns for the iron–azobenzene thin-film samples recorded after the deposition and after each humidity treatment and UV irradiation. c) FTIR spectra for a humidity-treated (1 month) sample and the same sample after being heat-treated for 15 min at different temperatures (45, 65, 85, and 90 °C).

irradiation could not be due to small changes in sample temperature by collecting FTIR spectra for a water-containing thin film first after a one-month humidity treatment, and then for the same film heated at different temperatures; Figure 3c shows that the water leaves the structure when the film is heated at 90 °C, but not below that temperature.

The FTIR spectra (Figure 3a) reveal further details concerning the water absorption/desorption process; upon the first humidity treatment a new band appears at 1690 cm^{-1} indicating the formation of free carboxylic acid groups. Simultaneously the intensity of the 1590 cm^{-1} carboxylate band somewhat decreases.[43,44] Hence it seems that some of the carboxylate groups are protonated upon the water absorption. We followed the water absorption/desorption cycles through GIXRD measurements (Figure 3b). The diffraction patterns remain otherwise very similar except for the changes seen after the first humidity treatment, indicating some initial modification in the crystal structure. In Figure 3b, the XRR-determined film density values are also given (in parentheses). It can be seen that the density of the original as-deposited iron–azobenzene film is 1.51 $g\,cm^{-3}$. Upon the first humidity treatment, when some of the carboxylate groups are protonated and the structure is slightly modified, the density decreases to 1.27 $g\,cm^{-3}$. After that, the density systematically increases to 1.35 $g\,cm^{-3}$ and decreases back to 1.27 $g\,cm^{-3}$ when water is desorbed and absorbed, respectively. We thus conclude that upon the repeated humidity-treatment/UV-illumination cycles when water is absorbed and desorbed significant changes in bonding/crystal structure occur only in the first water absorption step when some protonated carboxylic acid groups are formed.

In conclusion, we fabricated crystalline iron-azobenzene thin films from gaseous $FeCl_3$ and azobenzene-4,4′-dicarboxylic acid precursors using the ALD/MLD technique. In this new metal–organic structure the azobenzene moieties are able to undergo the *trans–cis* photoisomerization upon UV irradiation. We tentatively attribute this to the fact that the films are polycrystalline and moreover supported by the substrate. Changes in the diffraction pattern were seen only after longer irradiation periods when the *trans*-to-*cis* transformation level exceeded ca. 20 %. Moreover the gas (water) absorption capability of the films was demonstrated. Then, most excitingly the release of the absorbed water molecules could be triggered by the *trans–cis* photoisomerization of the azobenzene moieties achieved upon a 15 min UV irradiation. We foresee that our work could pave the way to the development of novel remote-controlled coatings dreamed of as enablers of many next-generation applications.

Acknowledgements

Funding was received from the European Research Council under the European Union's Seventh Framework Programme (FP/2007-2013)/ERC Advanced Grant Agreement (339478) and the Academy of Finland (296299). We acknowledge the RawMatTERS Finland infrastructure at Aalto Univ., and Dr. Jani Sainio and Dr. Ramesh Raju for the XPS and AFM measurements.

Conflict of interest

The authors declare no conflict of interest.

Keywords: atomic layer deposition · azobenzene · metal–organic frameworks · molecular layer deposition · thin films

How to cite: *Angew. Chem. Int. Ed.* **2019**, *58*, 13400–13404
Angew. Chem. **2019**, *131*, 13534–13538

[1] O. Shekhah, J. Liu, R. A. Fischer, C. Wöll, *Chem. Soc. Rev.* **2011**, *40*, 1081–1106.
[2] A. Schoedel, M. Li, D. Li, M. O'Keeffe, O. M. Yaghi, *Chem. Rev.* **2016**, *116*, 12466–12535.
[3] K. Ikigaki, K. Okada, Y. Tokudome, T. Toyao, P. Falcaro, C. J. Doonan, M. Takahashi, *Angew. Chem. Int. Ed.* **2019**, *58*, 6886–6890; *Angew. Chem.* **2019**, *131*, 6960–6964.
[4] J. J. Gassensmith, H. Furukawa, R. A. Smaldone, R. S. Forgan, Y. Y. Botros, O. M. Yaghi, J. F. Stoddart, *J. Am. Chem. Soc.* **2011**, *133*, 15312–15315.
[5] M. Ding, R. W. Flaig, H.-L. Jiang, O. M. Yaghi, *Chem. Soc. Rev.* **2019**, *48*, 2783–2828.
[6] H. Furukawa, K. E. Cordova, M. O'Keeffe, O. M. Yaghi, *Science* **2013**, *341*, 1230444.
[7] R. J. Kuppler, D. J. Timmons, Q. R. Fang, J. R. Li, T. A. Makal, M. D. Young, D. Yuan, D. Zhao, W. Zhuang, H. C. Zhou, *Coord. Chem. Rev.* **2009**, *253*, 3042–3066.
[8] M. M. Russew, S. Hecht, *Adv. Mater.* **2010**, *22*, 3348–3360.
[9] H. M. D. Bandara, S. C. Burdette, *Chem. Soc. Rev.* **2012**, *41*, 1809–1825.
[10] C. R. Crecca, A. E. Roitberg, *J. Phys. Chem. A* **2006**, *110*, 8188–8203.
[11] C. L. Jones, A. J. Tansell, T. L. Easun, *J. Mater. Chem. A* **2016**, *4*, 6714–6723.
[12] A. B. Kanj, K. Müller, L. Heinke, *Macromol. Rapid Commun.* **2018**, *39*, 1700239.
[13] L. T. M. Hoang, L. H. Ngo, H. L. Nguyen, H. T. H. Nguyen, C. K. Nguyen, B. T. Nguyen, Q. T. Ton, H. K. D. Nguyen, K. E. Cordova, T. Truong, *Chem. Commun.* **2015**, *51*, 17132–17135.
[14] R. Lyndon, K. Konstas, B. P. Ladewig, P. D. Southon, P. C. J. Kepert, M. R. Hill, *Angew. Chem. Int. Ed.* **2013**, *52*, 3695–3698; *Angew. Chem.* **2013**, *125*, 3783–3786.
[15] J. Park, D. Yuan, K. T. Pham, J. R. Li, A. Yakovenko, H. C. Zhou, *J. Am. Chem. Soc.* **2012**, *134*, 99–102.
[16] X. Yu, Z. Wang, M. Buchholz, N. Füllgrabe, S. Grosjean, F. Bebensee, S. Bräse, C. Wöll, L. Heinke, *Phys. Chem. Chem. Phys.* **2015**, *17*, 22721–22725.
[17] D. Hermann, H. A. Schwartz, M. Werker, D. Schaniel, U. Ruschewitz, *Chem. Eur. J.* **2019**, *25*, 3606–3616.
[18] K. Müller, J. Wadhwa, J. Singh Malhi, L. Schöttner, A. Welle, H. Schwartz, D. Hermann, U. Ruschewitz, L. Heinke, *Chem. Commun.* **2017**, *53*, 8070–8073.
[19] S. Castellanos, F. Kapteijn, J. Gascon, *CrystEngComm* **2016**, *18*, 4006–4012.
[20] F. X. Coudert, *Chem. Mater.* **2015**, *27*, 1905–1916.
[21] C. Liu, W. Zhang, Q. Zeng, S. Lei, *Chem. Eur. J.* **2016**, *22*, 6768–6773.
[22] J. Zhang, L. Wang, N. Li, J. Liu, W. Zhang, Z. Zhang, N. Zhou, X. Zhu, *CrystEngComm* **2014**, *16*, 6547–6551.
[23] A. Carné, C. Carbonell, I. Imaz, D. Maspoch, *Chem. Soc. Rev.* **2011**, *40*, 291–305.
[24] A. Bétard, R. A. Fischer, *Chem. Rev.* **2012**, *112*, 1055–1083.
[25] X. Meng, *J. Mater. Chem. A* **2017**, *5*, 18326–18378.
[26] T. Suntola, *Mater. Sci. Rep.* **1989**, *4*, 261–312.
[27] S. M. George, *Chem. Rev.* **2010**, *110*, 111–131.

[28] E. Ahvenniemi, M. Karppinen, *Chem. Commun.* **2016**, *52*, 1139 – 1142.
[29] E. Ahvenniemi, M. Karppinen, *Chem. Mater.* **2016**, *28*, 6260 – 6265.
[30] M. Nisula, M. Karppinen, *Nano Lett.* **2016**, *16*, 1276 – 1281.
[31] J. Penttinen, M. Nisula, M. Karppinen, *Chem. Eur. J.* **2017**, *23*, 18225 – 18231.
[32] J. L. Zhuang, K. Lommel, D. Ceglarek, I. Andrusenko, U. Kolb, S. Maracke, U. Sazama, M. Fröba, A. Terfort, *Chem. Mater.* **2011**, *23*, 5366 – 5374.
[33] T. Sato, Y. Ozaki, *Langmuir* **1994**, *10*, 2363 – 2369.
[34] J. W. Brown, B. L. Henderson, M. D. Kiesz, A. C. Whalley, W. Morris, S. Grunder, H. Deng, H. Furukawa, J. I. Zink, J. F. Stoddart, et al., *Chem. Sci.* **2013**, *4*, 2858 – 2864.
[35] J. Han, D. Yan, W. Shi, J. Ma, H. Yan, M. Wei, D. G. Evans, X. Duan, *J. Phys. Chem. B* **2010**, *114*, 5678 – 5685.
[36] T. Yamashita, P. Hayes, *Appl. Surf. Sci.* **2008**, *254*, 2441 – 2449.
[37] S. Saremi-Yarahmadi, K. G. U. Wijayantha, A. A. Tahir, B. Vaidhyanathan, *J. Phys. Chem. C* **2009**, *113*, 4768 – 4778.
[38] A. P. Grosvenor, B. A. Kobe, M. C. Biesinger, N. S. McIntyre, *Surf. Interface Anal.* **2004**, *36*, 1564 – 1574.
[39] M. Juppo, P. Alen, M. Ritala, M. Leskelä, *Chem. Vap. Deposition* **2001**, *7*, 211 – 217.
[40] P. Alén, M. Juppo, M. Ritala, T. Sajavaara, J. Keinonen, M. Leskelä, *J. Electrochem. Soc.* **2001**, *148*, G566 – G571.
[41] A. Khayyami, M. Karppinen, *Chem. Mater.* **2018**, *30*, 5904 – 5911.
[42] X. Xue, J. Zhu, Z. Zhang, N. Zhou, X. Zhu, *React. Funct. Polym.* **2010**, *70*, 456 – 462.
[43] J. B. Decoste, G. W. Peterson, B. J. Schindler, K. L. Killops, M. A. Browe, J. J. Mahle, *J. Mater. Chem. A* **2013**, *1*, 11922 – 11932.
[44] J. B. Decoste, G. W. Peterson, H. Jasuja, T. G. Glover, Y. G. Huang, K. S. Walton, *J. Mater. Chem. A* **2013**, *1*, 5642 – 5650.

Manuscript received: July 1, 2019
Accepted manuscript online: July 18, 2019
Version of record online: August 13, 2019

